 ©2017 Kvantovaya Elektronika and Turpion Ltd

X-RAY OPTICS

https://doi.org/10.1070/QEL16261

Imaging diffraction VLS spectrometer for a wavelength range $\lambda > 120$ Å

E.A. Vishnyakov, A.O. Kolesnikov, A.A. Kuzin, D.V. Negrov, E.N. Ragozin, P.V. Sasorov, A.N. Shatokhin

Abstract. **A broadband stigmatic (imaging) soft X-ray ($\lambda > 120$ Å) spectrometer is experimentally realised. The optical configuration of the spectrometer comprises a plane grazing-incidence reflection grating with a spacing varying across its aperture according to a preassigned law [a so-called varied line-space (VLS) grating] and a broadband spherical normal-incidence mirror with an aperiodic Mo/Si multilayer structure. The average plate scale amounts to ~5.5 Å mm^{-1}. The radiation is recorded with a matrix CCD detector (2048 × 1024 pixels of size 13 μm). The line spectra of the multiply charged ions LiIII and FV–FVII excited in laser-produced plasma are recorded with a spatial resolution of ~26 μm and a spectral resolving power $R \approx 500$ is experimentally demonstrated.**

Keywords: *soft X-ray range, stigmatic (imaging) spectrometer, VLS grating, aperiodic multilayer mirror, laser-produced plasma.*

1. Introduction

The task of constructing spectral images and, as a special case, of obtaining line spectra with a special resolution in the soft X-ray (SXR) range arises in the investigation of laboratory and astrophysical plasmas, as well as in the characterisation of laboratory SXR radiation sources. In recent years, the list of traditional objects of investigation (laser-produced plasma, plasmas of fast electric discharges, fast capillary discharge, etc.) was supplemented with several new ones. The cases in point are, in particular, cluster plasmas [1], the source of high-order harmonics in a relativistic laser plasma generated by a multiterawatt femtosecond laser [2] and the generation of SXR radiation in the reflection of Ti:sapphire laser radiation from the relativistic plasma wave driven by the multiterawatt laser in a pulsed helium jet (a relativistic 'flying mirror') [3], and the so-called 'warm dense matter' (WDM) produced by the pulse of an X-ray free-electron laser (XFEL) [4].

Frequently, the requirements to the spatial resolution of spectrometers are rather high: several experiments call for a spatial resolution of ~10 and even ~1 μm. In particular, Kando et al. [3] determined that the dimension of the 'flying mirror' region radiating in a spectral range of 12–20 nm does not exceed 16 μm. In Ref. [2], in which the harmonic 'comb' ranged into the 'water window' domain, it was theoretically shown by particle-in-cell (PIC) simulations that the harmonic generation under relativistic self-focusing conditions took place within a volume $\sim 10\lambda_0$ in diameter (λ_0 is the wavelength of the driving laser), with electron density singularities (peaks) occurring within this volume and being responsible for the high-order harmonic generation of highest intensity. To produce WDM plasma in Ref. [4], XFEL radiation pulses (λ = 13.5 nm, $\hbar\omega$ = 91.8 eV) were focused on an aluminium target to a spot 30 μm in diameter and the WDM plasma radiation was recorded with a spectral resolution of 0.2 nm with the use of a spectrometer with a free-standing transmission diffraction grating. Lastly, Pikuz et al. [5] experimentally showed that the XFEL radiation with an energy $\hbar\omega$ = 10.1 keV (the case in point is the SACLA XFEL, Japan) may be focused to a spot ~1 μm in diameter. Therefore, there objectively exists a demand for high-resolution SXR instruments that simultaneously provide spectral and spatial information about an object.

The task of obtaining spectra with one-coordinate spatial resolution and constructing spectral images is solved by an imaging (stigmatic) diffraction spectrometer. There are several versions of such spectrometer configurations. First, the case in point is the combination of a focusing normal-incidence multilayer mirror (MM) in combination with a free-standing diffraction grating (see, for instance, reviews [6, 7]). Among the drawbacks of this configuration is the relatively low limiting resolving power ($\lambda/\delta\lambda \approx 200$–$300$) attainable with this grating. Furthermore, the spectral image is modified by the support structure of the grating, be it a regular structure or quasi-random one. Another configuration version makes use of a spherical multilayer diffraction grating employed at near-normal radiation incidence, which possesses moderate astigmatism [8]. With the use of this grating it is possible to obtain a high spectral resolution but not a high spatial resolution. An exception is provided by the Wadsworth mount of a spherical grating, which provides a high angular resolution at a fixed wavelength. This mount has been repeatedly used in solar astronomy [9].

E.A. Vishnyakov P.N. Lebedev Physics Institute, Russian Academy of Sciences, Leninsky prosp. 53, 119991 Moscow, Russia; e-mail: juk301@mail.ru;
A.O. Kolesnikov, E.N. Ragozin, A.N. Shatokhin P.N. Lebedev Physics Institute, Russian Academy of Sciences, Leninsky prosp. 53, 119991 Moscow, Russia; Moscow Institute of Physics and Technology (State University), Institutskii per. 9, 141701 Dolgoprudnyi, Moscow region, Russia; e-mail: enragozin@gmail.com;
A.A. Kuzin Moscow Institute of Physics and Technology (State University), Institutskii per. 9, 141701 Dolgoprudnyi, Moscow region, Russia; Institute for Spectroscopy, Russian Academy of Sciences, ul. Fizicheskaya 5, Troitsk, 108840 Moscow, Russia;
D.V. Negrov Moscow Institute of Physics and Technology (State University), Institutskii per. 9, 141701 Dolgoprudnyi, Moscow region, Russia;
P.V. Sasorov M.V. Keldysh Institute of Applied Mathematics, Russian Academy of Sciences, Miusskaya square 4, 125047 Moscow, Russia

Received 28 November 2016
Kvantovaya Elektronika **47** (1) 54–57 (2017)
Translated by E.N. Ragozin

At present, gaining popularity are SXR spectrometer configurations based on reflection diffraction gratings whose line spacing varies across the aperture (VLS gratings). By directing a homocentric beam onto a VLS grating at a grazing incidence angle it is possible to obtain a stigmatic image at a fixed wavelength [10]. This configuration, in which the converging homocentric beam was produced by an X-ray telescope made up of figures of rotation, was employed to obtain a map of galactic and extragalactic radiation sources in the far VUV spectral region [11]. Recently, it was theoretically shown that a stigmatic VLS spectrometer configuration can be made using the combination of a concave VLS grating and a crossed focusing multilayer mirror [12].

In Ref. [13] we came up with the idea of a broadband imaging VLS spectrometer which combines the advantages of a normal-incidence broadband multilayer mirror and a plane VLS grating, as well as satisfies the stigmatic condition simultaneously at two wavelengths and the condition of practical stigmatism throughout a broad spectral interval (no less than an octave in wavelength). Our report is concerned with the implementation of this idea.

2. Spectrometer configuration

Let the spatial line density of a plane VLS grating be described by a polynomial dependence on the coordinate w (Fig. 1):

$$p(w) = p_0 + p_1 w + p_2 w^2 + p_3 w^3 + \ldots, \tag{1}$$

with $p(w) = \mathrm{d}n/\mathrm{d}w$, where n is the line number and p_0 is the line density at the centre of the aperture. As is well known, coefficient p_1 modifies the curve which describes the location of the horizontal (spectral) focus, while coefficients p_2 and p_3 affect the aberration of meridional coma and the spherical aberration, respectively [12]. Let a slightly astigmatic beam be incident on the VLS grating, L_h denote the distance of its horizontal focus from the grating centre, L_v be the distance of its vertical focus from the grating centre, φ be the grazing incidence angle for the central ray, and ψ be the wavelength-dependent grazing diffraction angle. Then, at a wavelength λ the direction ψ of central ray diffraction, the distances to the paraxial horizontal r'_h and vertical r'_v foci are described by the well-known equations:

$$\cos\varphi - \cos\psi = m\lambda p_0, \tag{2}$$

$$-\frac{\sin^2\varphi}{L_\mathrm{h}} + \frac{\sin^2\psi}{r'_\mathrm{h}} = m\lambda p_1, \tag{3}$$

$$r'_\mathrm{v} = L_\mathrm{v}, \tag{4}$$

where m is the order of diffraction. Under the notation adopted above, all distances and angles are assumed to be positive. The condition for achieving stigmatism ($r'_\mathrm{h} = r'_\mathrm{v}$) gives

$$\frac{L_\mathrm{h}\sin^2\psi}{\sin^2\varphi + mp_1\lambda L_\mathrm{h}} = L_\mathrm{v}. \tag{5}$$

Equation (5) in combination with Eqn (2) expresses the stigmatic condition at a wavelength λ. We express p_1 from Eqn (5) to obtain the relation between p_0 and φ_0, which arises when we require the elimination of astigmatism at two (λ_1 and λ_2) wavelengths:

$$p_1 = \frac{1}{m\lambda_1}\left[-\frac{\sin^2\varphi}{L_\mathrm{h}} + \frac{\sin^2\psi_1}{L_\mathrm{v}}\right] = \frac{1}{m\lambda_2}\left[-\frac{\sin^2\varphi}{L_\mathrm{h}} + \frac{\sin^2\psi_2}{L_\mathrm{v}}\right]. \tag{6}$$

Therefore, astigmatism can be eliminated simultaneously at two wavelengths when we sacrifice one of the free parameters – either p_0 or φ_0. Proceeding from the assumption that p_0 takes on one of customary values (for instance, 600 lines mm^{-1}), we define the value of p_0 and find the value

$$\varphi_0 = \arcsin\left(mp_0\sqrt{\lambda_1\lambda_2}\Big/\sqrt{L_\mathrm{v}/L_\mathrm{h} - 1}\right). \tag{7}$$

Parameters p_i ($i = 2, 3, \ldots$) of the plane VLS grating may be derived by expanding the following expression in a Taylor series:

$$mp(w)\lambda_\mathrm{opt} = \cos\left[\operatorname{arccot}\left(\cot\varphi_0 - \frac{w}{L_\mathrm{h}\sin\varphi_0}\right)\right] - \cos\left[\operatorname{arccot}\left(\cot\psi_\mathrm{opt} - \frac{w}{L_\mathrm{v}\sin\psi_\mathrm{opt}}\right)\right]. \tag{8}$$

Here, λ_opt is the wavelength of aberration compensation, $\lambda_\mathrm{opt} = \lambda_1$ in our case.

The optical configuration of the broadband stigmatic (imaging) spectrometer is depicted in Fig. 1. The drawing shows the paths of rays lying in the principal plane, which passes through the grating centre and is perpendicular to the grating lines.

The source (laser-produced plasma) is located in front of the entrance slit. The beam of rays transmitted through the entrance slit is reflected from the concave spherical MM (R = 1 m) whose coating is an aperiodic structure with a nearly uniform reflectivity in the 125–250 Å spectral range [14]; the incidence angle of the central ray of the beam makes an angle of approximately 8° with the normal. The beam of rays reflected from the MM is directed to the VLS grating mounted at a grazing incidence angle. The spatial line density at the grating centre is p_0 = 600 lines mm^{-1}. Proceeding from the mirror-defined spectral interval, in the calculations we adopted λ_1 = 144 Å and λ_2 = 270 Å, which minimised the geometrical defocusing in the specified range; in this case, $\varphi_0 = 6.44°$ and p_1 = 2.37 mm^{-2}.

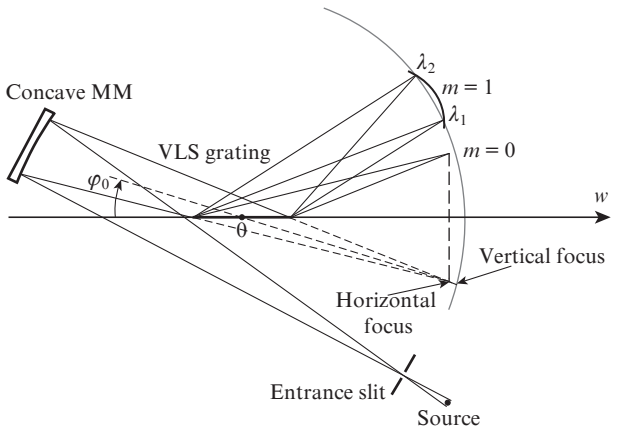

Figure 1. Optical configuration of the imaging spectrometer.

The arc in Fig. 1 belongs to the circle of radius L_v drawn about the grating centre, where L_v is the distance of the grating centre from the vertical focus of the source image produced by the mirror. The distance between the grating centre and the horizontal focus of the image of the entrance slit is denoted by L_h. In the first diffraction order ($m = 1$) the horizontal focal curve intersects the arc of the vertical focal circle at two points ($\lambda_1 = 144$ Å, $\lambda_2 = 270$ Å). Therefore, in the portion of the circular arc there forms the spectrum of the source with spatial resolution in the direction parallel to the entrance slit. The spectrometer plate scale amounts to 5.4 Å mm^{-1} in the short-wavelength side of the spectrum and to 5.8 Å mm^{-1} in the long-wavelength one. The radiation was recorded using a backside-illuminated matrix CCD detector (2048 × 1024 pixels of size 13 μm each, with a sensitive area length of 27 mm).

The VLS grating was fabricated by electron-beam lithography (EBL) followed by plasmachemical etching. A 100-nm-thick tungsten film was deposited on a glass substrate. Then it was spin-coated with the e-beam resist PMMA 4 (Microchem) at 5000 rpm. The resist was exposed to the electron beam with the following parameters: beam energy 50 keV, current 15.5 nA, write-field 600 × 600 μm, dwell time 0.14 ms. The resist was developed in the isopropyl alcohol solution of methyl isobutyl ketone (MIBK : IPA = 1:3) for 120 s and then placed in isopropyl alcohol for 60 s. Eventually the grating was formed by SF_6 plasmachemical etching through the resist mask. After the etching, the resist was removed in an oxygen plasma.

Figure 2 shows the photograph of the spectrometer, whose elements are accommodated on a duralumin plate of size 1100 × 600 mm. The coefficient p_1, which characterises the line density gradient across the aperture, was equal to 2.32 lines mm^{-2}, which was sufficiently close to the design value (2.37 lines mm^{-2}) to make possible the spectrometer alignment by way of a small correction of the angles and distances. To this end, the VLS grating mount was attached to a motorised rotary stage and the CCD detector was attached to a motorised translation stage. The spectrograph was placed in a vacuum chamber measuring 3.8 × 0.9 m evacuated to a pressure of 5×10^{-5} Torr. The motorised stages were controlled with a computer, which also displayed the recorded spectral image.

The laser plasma was produced by focusing the pulse of neodymium laser radiation (0.5 J energy on the target, 10 ns pulse duration) on a plane rotary target, whose surface lay in the principal plane of the spectrometer. The optical configuration was designed in such a way that the detector plane coincided with the horizontal (spectral) focus of the image of the entrance slit and with the vertical focus of the image of the

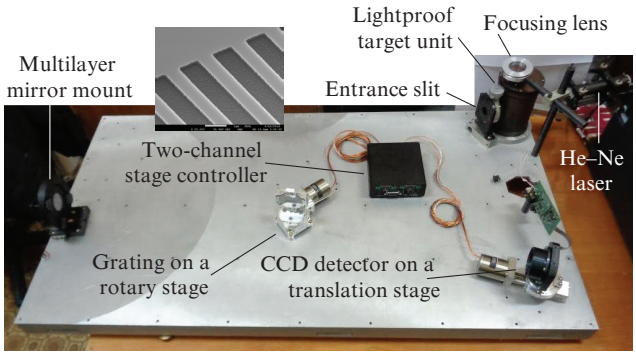

Figure 2. Elements of the imaging spectrometer accommodated on a duralumin plate. The inset shows a portion of the tungsten grating.

laser-produced plasma. This ensured that the instrument possessed both spectral and spatial resolution, thereby yielding the dependence of spectral line intensities on the distance from the target surface (from the light-shadow boundary).

Due to its stigmatism, the instrument exhibited a high light efficiency: the spectrum in a range of 120–210 Å was recorded in one laser shot (Fig. 3). The portion of the spectrum in Fig. 3 contains lines of the ions LiIII and FV–FVII. In the spectrum of a LiF target the strongest line (FVII, 3d → 2p, the doublet 127.65 and 127.80 Å) saturates those detector pixels which have to record the radiation of the near-surface (brightest) plasma. The second spectral order is much weaker than the first one, which would be expected for a laminar grating with a duty ratio of about 0.5. With increasing wavelength, the spectral line intensities and the CCD detector responsivity become lower.

The width of the entrance slit was equal to 30 μm. In this case, the line full widths at half maximum (FWHM) fall on four detector pixels (52 μm). In view of the plate scale (5.4 Å mm^{-1} in the short-wavelength side of the spectrum and 5.8 Å mm^{-1} in long-wavelength one), this corresponds to a resolving power of ~450 and ~600. The closest lines that are safely resolved in the first diffraction order are the 163.138 Å line of the ion FVI and the unresolved line group {163.456, .501, .558, .596 Å} of FV, which gives $\lambda/\delta\lambda \approx 510$. Therefore, this is a demonstration of a spectral resolving power of ~500 (a conservative estimate). The doublet line 3d → 2p (127.65 and 127.80 Å) of the ion FVII is safely resolved in the second order, testifying to a resolving power of ~900. The spatial resolution (vertically) estimated at light-shadow boundary corresponds to two detector pixels, which amounts to 26 μm.

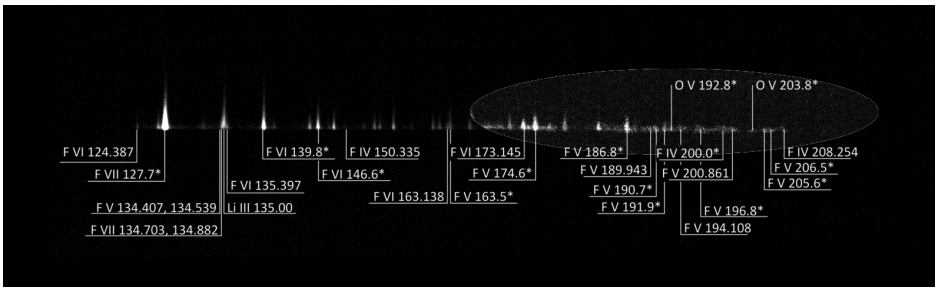

Figure 3. First-order stigmatic spectrum of the multiply charged ions of lithium and fluorine recorded in one laser shot (0.5 J, 10 ns). Asterisks indicate groups of unresolved lines.

3. Conclusions

A broadband stigmatic spectrometer for a wavelength range of 120–250 Å was experimentally realised for the first time, which comprises an aperiodic normal-incidence multilayer mirror and a plane grazing-incidence VLS grating made by electron-beam lithography technique. For a detector, use was made of a matrix CCD detector with pixels of size 13 μm and a sensitive area length of 27 mm. The spectrometer efficiency was demonstrated in the recording of laser-produced plasma spectra: the spectrum of a LiF target was recorded in one laser shot (0.5 J, 10 ns). The spatial resolution was equal to 26 μm and the spectral resolving power amounted to 500. Further improvement of the spectrometer characteristics will be possible after improvement of the technology of VLS-grating fabrication.

Acknowledgements. This work was supported by the Russian Science Foundation (Grant No. 14-12-00506).

References

1. Faenov A.Ya., Oks E., Dalimier E., et al. *Kvantovaya Elektron.*, **46** (4), 338 (2016) [*Quantum Electron.*, **46** (4), 338 (2016)].
2. Pirozhkov A.S., Kando M., Esirkepov T.Zh., et al. *Phys. Rev. Lett.*, **108**, 135004 (2012).
3. Kando M., Pirozhkov A.S., Kawase K., et al. *Phys. Rev. Lett.*, **103**, 235003 (2009).
4. Zastrau U., Fortmann C., Fäustlin R.R., et al. *Phys. Rev. E*, **78**, 066406 (2008).
5. Pikuz T., Faenov A., Matsuoka T., et al. *Conf. Program and Book of Abst. 15th Int. Conf. on X-Ray Lasers 2016 (ICXRL2016)* (Nara, Japan, 22–27 May 2016) p. 75.
6. Pirozhkov A.S., Ragozin E.N. *Usp. Fiz. Nauk*, **185** (11), 1203 (2015) [*Phys. Usp.*, **58** (11), 1095 (2015)].
7. Vishnyakov E.A., Kamenets F.F., Kondratenko V.V., et al. *Kvantovaya Elektron.*, **42** (2), 143 (2012) [*Quantum Electron.*, **42** (2), 143 (2012)].
8. Kowalski M.P., Seely J.F., Cruddace R.G., et al. *Proc. SPIE Int. Soc. Opt. Eng.*, **1945**, 164 (1993).
9. Tousey R., Bartoe J.-D.F., Brueckner G.E., Purcell J.D. *Appl. Opt.*, **16** (4), 870 (1977).
10. Hettrick M.C., Bowyer S. *Appl. Opt.*, **22** (24), 3921 (1983).
11. Hettrick M.C., Bowyer S., Malina R.F., et al. *Appl. Opt.*, **24** (12), 1737 (1985).
12. Vishnyakov E.A., Kolesnikov A.O., Ragozin E.N., Shatokhin A.N. *Kvantovaya Elektron.*, **46** (10), 953 (2016) [*Quantum Electron.*, **46** (10), 953 (2016)].
13. Vishnyakov E.A., Ragozin E.N., Shatokhin A.N. *Kvantovaya Elektron.*, **45** (4), 371 (2015) [*Quantum Electron.*, **45** (4), 371 (2015)].
14. Vishnyakov E.A., Mednikov K.N., Pertsov A.A., et al. *Kvantovaya Elektron.*, **39** (5), 474 (2009) [*Quantum Electron.*, **39** (5), 474 (2009)].